A Directly Fused Tetrameric Porphyrin Sheet and Its Anomalous Electronic Properties That Arise from the Planar Cyclooctatetraene Core

ARTICLE *in* JOURNAL OF THE AMERICAN CHEMICAL SOCIETY · APRIL 2006

Impact Factor: 12.11 · DOI: 10.1021/ja057812l · Source: PubMed

13 AUTHORS, INCLUDING:

Takuya Matsumoto
Graduate School of Science, Osaka University
108 PUBLICATIONS **1,750** CITATIONS
SEE PROFILE

Deok Yun Kim
OCI Company
7 PUBLICATIONS **562** CITATIONS
SEE PROFILE

Dongho Kim
Yonsei University
496 PUBLICATIONS **13,380** CITATIONS
SEE PROFILE

Nagao Kobayashi
Tohoku University
529 PUBLICATIONS **11,352** CITATIONS
SEE PROFILE

J|A|C|S
ARTICLES
Published on Web 03/08/2006

A Directly Fused Tetrameric Porphyrin Sheet and Its Anomalous Electronic Properties That Arise from the Planar Cyclooctatetraene Core

Yasuyuki Nakamura,[†] Naoki Aratani,[†] Hiroshi Shinokubo,[†] Akihiko Takagi,[‡] Tomoji Kawai,[‡] Takuya Matsumoto,[‡] Zin Seok Yoon,[||] Deok Yun Kim,[||] Tae Kyu Ahn,[||] Dongho Kim,*[,||] Atsuya Muranaka,[§] Nagao Kobayashi,*[,§] and Atsuhiro Osuka*[,†]

Contribution from the Department of Chemistry, Graduate School of Science, Kyoto University, and CREST, Japan Science and Technology Agency, Sakyo-ku, Kyoto 606-8502, Japan, The Institute of Scientific and Industrial Research, Osaka University, and CREST, Japan Science and Technology Agency, Mihogaoka, Ibaragi, Osaka 567-0047, Japan, Department of Chemistry, Graduate School of Science, Tohoku University, Aoba-ku, Sendai 980-8578, Japan, and Center for Ultrafast Optical Characteristics Control and Department of Chemistry, Yonsei University, Seoul 120-749, Korea

Received November 30, 2005; E-mail: osuka@kuchem.kyoto-u.ac.jp; dongho@yonsei.ac.kr; nagaok@mail.tains.tohoku.ac.jp

Abstract: Oxidation of a directly meso−meso linked cyclic porphyrin tetramer **2** gave a porphyrin sheet **3**. The symmetric square structure of **3** is indicated by its simple ^{1}H NMR spectrum that exhibits only two signals for the porphyrin β-protons. The absorption spectrum of **3** displays characteristic Soret-like broad bands and weak Q-bands, and its magnetic circular dichroism (MCD) spectrum exhibits a negative Faraday *A* term at the 762 nm band as a rare case, indicating the absorption as a transition from a nondegenerate level to a degenerate level. A slightly longer S_1-state (1.1 ps) and smaller TPA cross section (2750 GM) than a tetrameric linear porphyrin tape also indicate its unique electronic properties. The porphyrin sheet **3** forms stable 1:2 complexes with guest molecules **G1** and **G2**, whose ^{1}H NMR spectra exhibit remarkable downfield shifts for the guest protons that are located just above the cyclooctatetraene (COT) core of **3**, whereas the imidazolyl protons bound to the zinc(II) porphyrin local cores are observed at slightly upfield positions. These results have been qualitatively accounted for in terms of the presence of a strong paratropic ring current around the COT core that propagates through the whole π-electronic network of **3**, hence competing with and canceling the weak diatropic ring currents of the local zinc(II) porphyrins. This explanation was supported by DFT calculation performed at the GIAO-B3LYP/6-31G* level, which indicated large positive NICS values within the COT core and small NICS values within the local zinc(II) porphyrins.

Introduction

Porphyrin is one of the most extensively studied macrocyclic systems, displaying rich coordination chemistry with various metal ions. Its 18π-conjugated electronic network in a square-planar circuit causes a strong aromatic diatropic ring current that is quite useful in host−guest chemistry, particularly for the identification of organic molecules ligated on the central metal of porphyrin. It is also known that the electronic nature of porphyrin is susceptible to peripheral functional modifications, which have, through introduction of π-conjugated segments at the porphyrinic periphery, been used for the creation of a variety of conjugated porphyrins and porphyrin oligomers that exhibit unique optical and electrochemical properties.[1]

In the past decade, we have explored various directly meso−meso linked porphyrin arrays on the basis of silver(I)-promoted coupling of a 5,15-diaryl substituted zinc(II) porphyrin.[2,3] These porphyrin arrays are promising as an optical molecular wire by transmitting captured excitation energy over a long distance.[4]

[†] Kyoto University and CREST.
[‡] Osaka University and CREST.
[§] Tohoku University.
[||] Yonsei University.

(1) Jaquinod, L. In *The Porphyrin Handbook*; Kadish, K. M., Smith, K. M., Guilard, R., Eds.; Academic Press: San Diego, 2000; Vol. 1, pp 201−237.

(2) (a) Osuka, A.; Shimidzu, H. *Angew. Chem., Int. Ed. Engl*. **1997**, *36*, 135. (b) Aratani, N.; Osuka, A.; Kim, Y. H.; Jeong, D. H.; Kim, D. *Angew. Chem., Int. Ed*. **2000**, *39*, 1458. (c) Nakano, A.; Osuka, A.; Yamazaki, I.; Yamazaki, T.; Nishimura, Y. *Angew. Chem., Int. Ed*. **1998**, *37*, 3023. (d) Nakano, A.; Yamazaki, T.; Nishimura, Y.; Yamazaki, I.; Osuka, A. *Chem.-Eur. J*. **2000**, *6*, 3254. (e) Kim, Y. H.; Jeong, D. H.; Kim, D.; Jeoung, S. C.; Cho, H. S.; Kim, S. K.; Aratani, N.; Osuka, A. *J. Am. Chem. Soc.* **2001**, *123*, 76. (f) Kim, D.; Osuka, A. *J. Phys. Chem. A* **2003**, *107*, 8791.

(3) (a) Susumu, K.; Shimidzu, T.; Tanaka, K.; Segawa, H. *Tetrahedron Lett.* **1996**, *37*, 8399. (b) Khoury, R. G.; Jaquinod, L.; Smith, K. M. *Chem. Commun*. **1997**, 1057. (c) Senge, M. O.; Feng, X. *Tetrahedron Lett*. **1999**, *40*, 4165. (d) Wojaczynski, J.; Latos-Grazynski, L.; Chmielewski, P. J.; Van Calcar, P.; Balch, A. L. *Inorg. Chem.* **1999**, *38*, 3040. (e) Shi, X.; Liebeskind, L. S. *J. Org. Chem*. **2000**, *65*, 1665. (f) Ogawa, K.; Kobuke, Y. *Angew. Chem., Int. Ed*. **2000**, *39*, 4070. (g) Imahori, H.; Tamaki, K.; Araki, Y.; Sekiguchi, Y.; Ito, O.; Sakata, Y.; Fukuzumi, S. *J. Am. Chem. Soc.* **2002**, *124*, 5165. (h) Bonifazi, D.; Diederich, F. *Chem. Commun.* **2002**, 2178. (i) Miller, M. A.; Lammi, R. K.; Prathapan, S.; Holten, D.; Lindsey, J. S. *J. Org. Chem*. **2000**, *65*, 6634. (j) Ottonelli, M. *Synth. Met*. **2003**, *138*, 173.

Scheme 1. Synthesis of **3**[a]

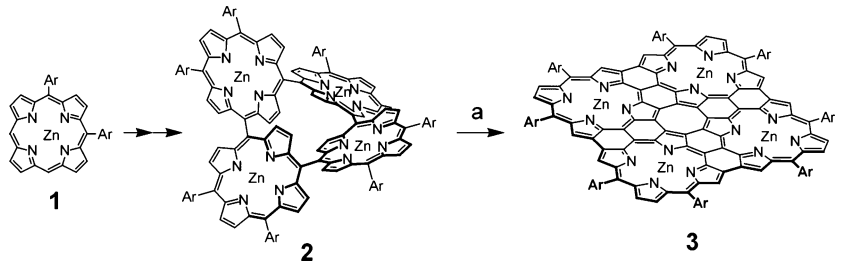

[a] Conditions: (a) DDQ, $Sc(OTf)_3$, toluene, 55 °C, 77%. Ar = 3,5-di-*tert*-butylphenyl.

Actually, the efficient excitation energy transfer (EET) is achieved over a long distance through meso−meso linked zinc(II) porphyrin arrays.[4] This function relies on their excitonically coupled but not fully π-conjugated electronic character. Further oxidation of singly meso−meso linked porphyrin arrays under stronger conditions (DDQ and $Sc(OTf)_3$) provided meso−meso, $\beta-\beta$, $\beta-\beta$ triply linked porphyrin arrays (porphyrin tapes),[5,6] whose Q-like bands, the lowest electronic absorption bands, exhibit continuous red-shifts, reaching deeply into the infrared region due to the extensive π-conjugation over the molecules. One-dimensionally extended π-conjugation causes a significant perturbation for the molecular orbital of porphyrins that breaks down the degeneracy of LUMOs. As a consequence, the lowest energy bands that correspond to formally forbidden Q-bands transition in the D_{4h}-symmetry zinc(II) porphyrin monomer are increasingly intensified upon the extension of the arrays.

In this paper, we report the synthesis and characterizations of a square-planar porphyrin sheet **3**, which is, to the best of our knowledge, the first example of two-dimensionally π-extended porphyrinic systems caused by symmetric direct fusion of four porphyrins. The molecule **3** is of great interest, because it allows for direct comparison of molecular morphology effects, linear versus square, upon the overall electronic properties of fused-conjugation of porphyrins. The electronic network of **3** consists of only porphyrins and thus is also interesting from a viewpoint of its analogy with those of polyacene and graphene analogues.[7] Anomalous electronic properties of **3** that differ significantly from those of usual porphyrins particularly in respect of aromaticity will be discussed in relation to the structural motif of its enforced planar cyclooctatetraene (COT) core.

Results and Discussion

Synthesis. Initially, we attempted to prepare porphyrin tetramer **3** by direct oxidative tetramerization of 5,10-diaryl zinc(II) porphyrin **1** with DDQ and $Sc(OTf)_3$. Analysis of this reaction mixture by matrix assisted laser desorption ionization time-of-flight mass spectroscopy (MALDI-TOF-MS) indicated the formation of **3**, which, however, could not be isolated in a pure form from this reaction mixture. In the next attempt, as a starting substrate, we employed directly meso−meso linked cyclic porphyrin tetramer **2** that was prepared from **1** through a stepwise coupling reaction sequence.[8] In toluene, **2** was treated with 30 equiv of DDQ and $Sc(OTf)_3$ at 55 °C for 5 h followed by separation over a short alumina column to provide **3** as black solids in 77% yield (Scheme 1). Inherent poor solubility of **3** can be improved by addition of a small amount of butylamine, which was quite important for its separation, final purification, and ^{1}H NMR measurements. MALDI-TOF-MS revealed the parent ion peak of **3** at m/z = 2977.4 [M^+] (calcd for $[C_{192}H_{184}N_{16}Zn_4]^+$ = 2977.2). In accord with the highly symmetric structure, the ^{1}H NMR spectrum of **3** in $CDCl_3$ containing 1% butylamine exhibited two singlets at 5.98 and 6.14 ppm for the porphyrin β-protons and a doublet at 7.01 ppm and a triplet at 7.29 ppm for the *ortho*- and *para*-protons of the meso-aryl substituents, respectively (Figure 1). The peripheral pyrrolic β-protons are observed at higher field as compared to those of the corresponding singly meso−meso linked porphyrin arrays[2] or linear porphyrin tapes,[9] which can be attributed to an attenuated diatropic ring current in **3**.

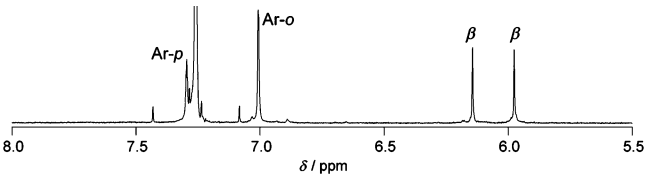

Figure 1. ^{1}H NMR spectrum of **3** in $CDCl_3$ containing 1% butylamine.

STM Measurements. Recently, we have succeeded in the STM detection of the dodecameric porphyrin wheel as discrete ring images.[10] By using the same pulse injection method, a dilute solution of **3** in $CHCl_3$ was sprayed onto clean flat Cu(100) surfaces that were obtained by cycles of annealing and Ar-ion sputtering.[11] In-situ STM measurements were performed at room temperature in ultrahigh vacuum ($<10^{-10}$ mbar) in a constant current mode. The STM images of **3** taken at a sample bias voltage of 1 V and a tunneling current of 3 pA revealed four spots arranged in a square manner with 3.2 × 3.2 nm^2 area, a peak-to-peak distance of 1.2 nm, and height of 0.21 nm (Figure 2).[12] Molecular size estimated from the STM image is roughly

(4) Aratani, N.; Cho, H. S.; Ahn, T. K.; Cho, S.; Kim, D.; Sumi, H.; Osuka, A. *J. Am. Chem. Soc*. **2003**, *125*, 9668.
(5) (a) Tsuda, A.; Furuta, H.; Osuka, A. *Angew. Chem., Int. Ed*. **2000**, 39, 2549. (b) Tsuda, A.; Furuta, H.; Osuka, A. *J. Am. Chem. Soc.* **2001**, *123*, 10304. (c) Tsuda, A.; Osuka, A. *Science* **2001**, *293*, 79. (d) Kamo, M.; Tsuda, A.; Nakamura, Y.; Aratani, N.; Furukawa, K.; Kato, T.; Osuka, A. *Org. Lett*. **2003**, *5*, 2079. (e) Nakamura, Y.; Aratani, N.; Tsuda, A.; Osuka, A.; Furukawa, K.; Kato, T. *J. Porphyrins Phthalocyanines* **2003**, *7*, 264. (f) Tsuda, A.; Nakamura, Y.; Osuka, A. *Chem. Commun*. **2003**, 1096.
(6) (a) Blake, I. M.; Krivokapic, A.; Katterle, M.; Anderson, H. L. *Chem. Commun*. **2002**, 1662. (b) Bonifazi, D.; Scholl, M.; Song, F.; Echegoyen, L.; Accorsi, G.; Armaroli, N.; Diederich, F. *Angew. Chem., Int. Ed*. **2003**, *42*, 4966.
(7) Watson, M. D.; Fechtenkötter, A.; Müllen, K. *Chem. Rev*. **2001**, *101*, 1267.
(8) Nakamura, Y.; Hwang, I.-W.; Aratani, N.; Ahn, T. K.; Ko, D. M.; Takagi, A.; Kawai, T.; Matsumoto, T.; Kim, D.; Osuka, A. *J. Am. Chem. Soc*. **2005**, *127*, 236.
(9) Ikeue, T.; Aratani, N.; Osuka, A. *Isr. J. Chem*. **2005**, *45*, 293.
(10) Peng, X.; Aratani, N.; Takagi, A.; Matsumoto, T.; Kawai, T.; Hwang, I.-W.; Ahn, T. K.; Kim, D.; Osuka, A. *J. Am. Chem. Soc.* **2004**, *126*, 4468.
(11) (a) Tanaka, H.; Nakagawa, T.; Kawai, T. *Surf. Sci*. **1996**, *364*, L575. (b) Takagi, A.; Yanagawa, Y.; Tsuda, A.; Aratani, N.; Matsumoto, T.; Osuka, A.; Kawai, T. *Chem. Commun*. **2003**, 2986.
(12) The estimated molecular width based on the calculated structure of *meso*-phenyl substituted **3** was ca. 2.7 nm.

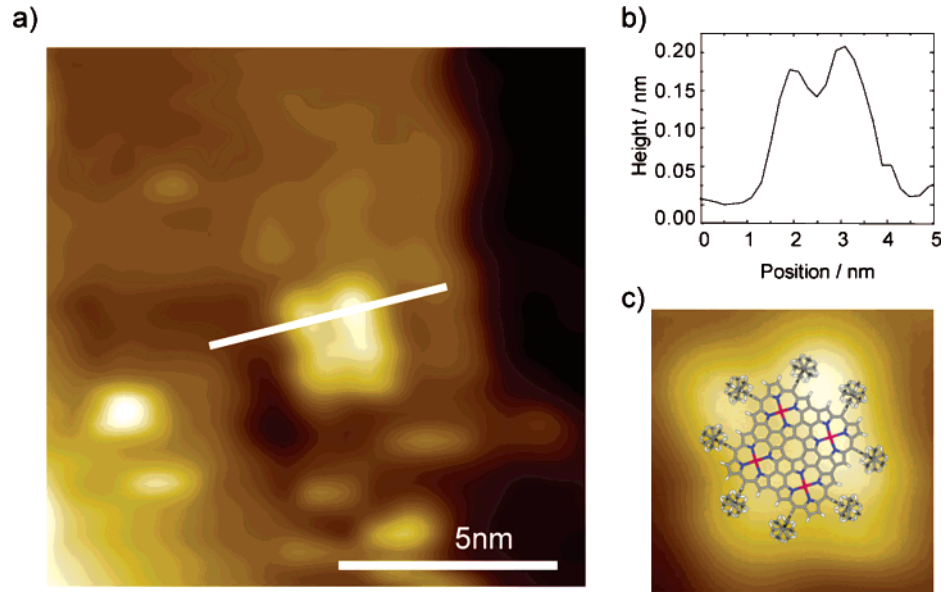

Figure 2. (a) STM images of **3**. (b) Height profile along the bar in (a). (c) An enlargement spot and molecular model.

consistent with the calculated structure, and observed bright spots have been assigned to two neighboring *meso*-di-*tert*-butylphenyl substituents as shown in Figure 2c. This assignment is in agreement with the previous STM studies on *meso*-(3,5-di-*tert*-butyl)phenyl porphyrins.[13]

UV−Vis Absorption and Magnetic Circular Dichroism Spectra. The porphyrin sheet **3** exhibits considerably broadened absorption bands in the wide range from UV−visible to near-IR (Figure 3a, bottom), which can be roughly divided into three distinct spectral regions, Band I (300−600 nm), Band II (600−1000 nm), and Band III (1000−1500 nm). Band III is considerably weaker as compared to that of one-dimensional tetrameric porphyrin tape. The magnetic circular dichroism (MCD) spectrum of **3** shows weak and intense signals for Bands I and II, respectively (Figure 3a, top). Because these spectral features have first derivative shapes, these signals can be assigned as Faraday *A* terms arising from transitions from a nondegenerate level to a degenerate level.[14] Notably, a distinct negative Faraday *A* term is observed for Band II, that is, positive/negative signs in ascending energy as a rare case,[15] which is in contrast to positive Faraday *A* terms that are usually observed for porphyrin skeletons. The MCD spectral pattern for the Band III region has been assigned as Faraday *B* terms, because the spectrum is similar to those of the absorption spectra, which indicates that the bands can be assigned as transitions between nondegenerate states. The absorption spectrum has been simulated using time-dependent Hartree−Fock theory based on the ZINDO/S Hamiltonian (TDHF-ZINDO/S) on *meso*-phenyl-substituted porphyrin sheet $\mathbf{3}_{Ph}$ as shown in Figure 3b.[16] Two intense absorption bands are predicted at 479 nm (oscillator strength $f = 2.930$) and 640

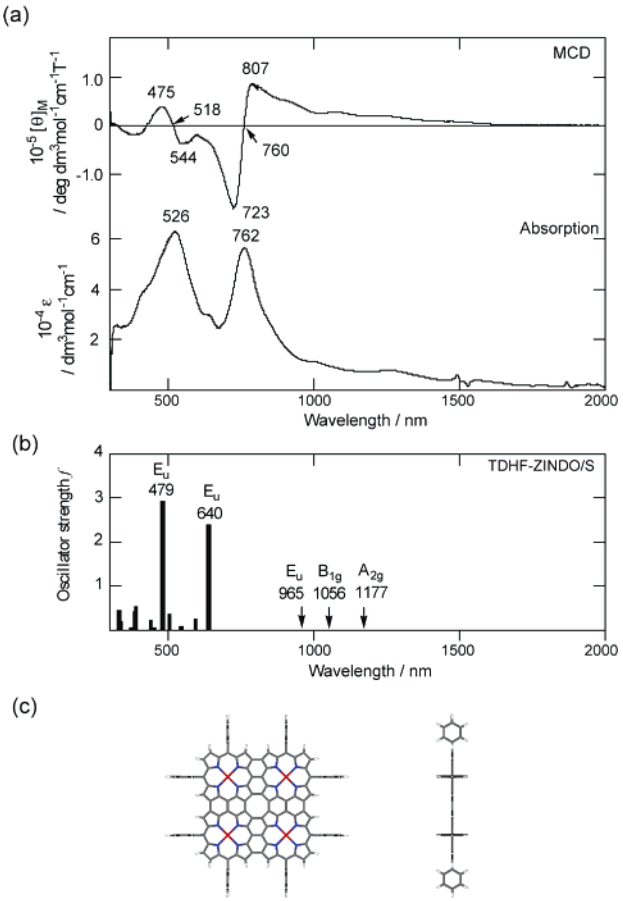

Figure 3. (a) Experimental MCD (top) and absorption (bottom) spectra of **3** recorded in pyridine-d_5 at room temperature. (b) Stick absorption spectrum of $\mathbf{3}_{Ph}$ calculated by TDHF-ZINDO/S method. (c) Calculated structure of $\mathbf{3}_{Ph}$; top view (left) and side view (right).

nm ($f = 2.377$), which can be assigned as the main electronic transitions of Bands I and II, respectively. The predicted excited states (E_u) are doubly degenerate, which leads to a prediction of Faraday *A* terms in the MCD spectrum. Two dipole-forbidden transitions (1177 nm (A_{2g}), $f = 0$ and 1056 nm (B_{1g}), $f = 0$) and an allowed transition with weak oscillator strength (965

(13) (a) Gimzewski, J. K.; Jung, T. A.; Cuberes, M. T.; Schlittler, R. R. *Surf. Sci.* **1997**, *386*, 101. (b) Yokoyama, T.; Yokoyama, S.; Kamikado, T.; Mashiko, S. *J. Chem. Phys.* **2001**, *115*, 3814. (c) Moresco, F.; Meyer, G.; Rieder, K.-H. *Phys. Rev. Lett.* **2001**, *86*, 672.
(14) (a) Michl, J. *J. Am. Chem. Soc.* **1978**, *100*, 6801. (b) Höweler, U.; Downing, J. W.; Fleischhauer, J.; Michl, J. *J. Chem. Soc., Perkin Trans. 2* **1998**, 1101. (c) Muranaka, A.; Yokoyama, M.; Matsumoto, Y.; Uchiyama, M.; Tsuda, A.; Osuka, A.; Kobayashi, N. *ChemPhysChem* **2005**, *6*, 171.
(15) Recently, negative Faraday *A* terms for the cyclo[*n*]pyrrole system have been reported. Gorski, A.; Köhler, T.; Seidel, D.; Lee, J. T.; Orzanowska, G.; Sessler, J. L.; Waluk, J. *Chem.-Eur. J.* **2005**, *11*, 4179.
(16) Nguyen, K. A.; Day, P. N.; Pachter, R.; Tretiak, S.; Chernyak, V.; Mukamel, S. *J. Phys. Chem. A* **2002**, *106*, 10285.

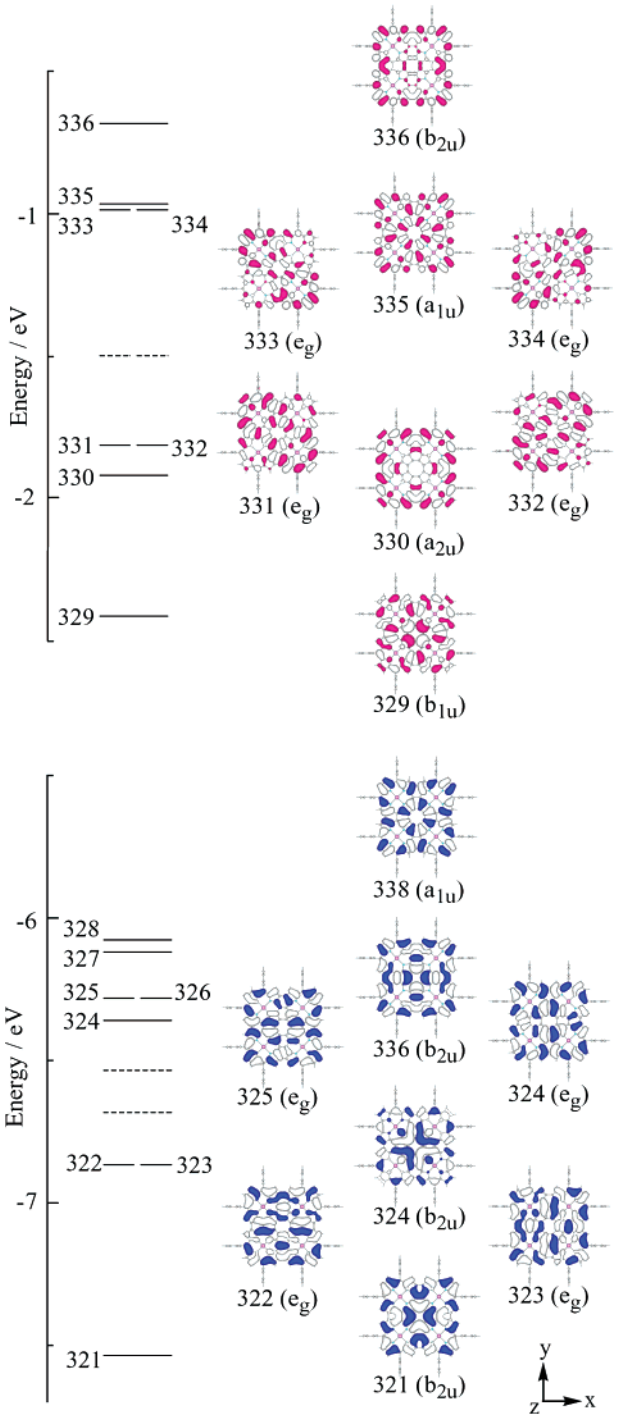

Figure 4. Frontier molecular orbital diagram and contour plots of occupied and virtual orbitals of $\mathbf{3}_{Ph}$ (TDHF-ZINDO/S). The dotted lines indicate four frontier molecular orbitals of D_{4h} zinc tetraphenylporphyrin (Zn-TPP).

nm (E_u), $f = 0.016$) are predicted in the Band III region. The broad and weak Faraday *B* terms observed for Band III can be associated with these three transitions, because absorption intensity could arise either from vibronic couplings or from a reduction of the ideal D_{4h} symmetry.

The origin of the unusual spectral features can be readily deduced from the orbital degeneracies of the frontier molecular orbitals (MOs) of the π-system (Figure 4). In the case of metalloporphyrins, the LUMO is typically orbitally degenerate (e_g) and the HOMOs are typically accidentally near degenerate (a_{1u} and a_{2u}).[17] In contrast, both the HOMO (328, a_{1u}) and the

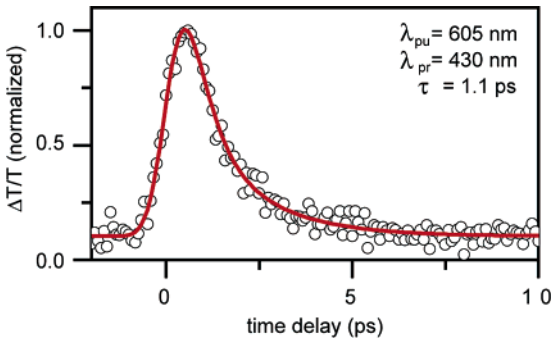

Figure 5. Excited-state dynamics of **3** in toluene containing 1% butylamine.

LUMO (329, b_{1u}) of $\mathbf{3}_{Ph}$ are nondegenerate. The low-energy Faraday *B* terms in the Band III region can be readily accounted for on this basis. The calculated 640 nm band is predicted to arise from a transition linking a degenerate orbital with a nondegenerate one (such as 322(323)→329 and 325(326)→330), whereas the 479 nm band is predicted to arise primarily from a transition linking a nondegenerate orbital and a degenerate one (i.e., electron-dominating transition). Negative Faraday *A* terms tend to arise from transitions in which orbital angular momentum (OAM) is greater in the ground state than in the excited state, while positive Faraday *A* terms are associated with transitions where OAM is greater in the excited state. Because the OAM associated with electron circulation would normally be anticipated to be greater within a degenerate orbital, the results obtained from the TDHF-ZINDO/S calculation are consistent with the positive and negative Faraday *A* terms observed for Bands I and II, respectively.

Excited-State Dynamics. With an increase in the number of porphyrins, linear porphyrin tapes exhibit a gradual red-shift of the lowest energy absorption band due to a decrease of the HOMO−LUMO energy gap, leading to a systematic decrease in the S_1-state lifetime from 4.5 ps (dimer) to 0.72 ps (tetramer).[18,19] The transient absorption decay profile of porphyrin sheet **3** ($\lambda_{pu} = 605$ nm, $\lambda_{pr} = 430$ nm) revealed a single-exponential decay of $\tau = 1.1$ ps (Figure 5), indicating that the S_1-state lifetime of **3** is remarkably reduced as compared to zinc(II) porphyrin monomer ($\tau = 2.4$ ns) but is slightly longer than that of the tetrameric porphyrin tape ($\tau = 0.72$ ps). In addition, we could not observe any transients in the nanosecond flash photolysis measurement, indicating inefficient triplet state formation. Therefore, the major relaxation pathway of the S_1-state of the porphyrin sheet **3** is believed to be an internal conversion process mainly due to a much reduced HOMO−LUMO energy gap as compared to zinc(II) porphyrin monomer.

Two-Photon Absorption Cross Section. The two-photon absorption (TPA) cross section (σ) of **3** was also measured, because the TPA values of organic molecules reflect the degree of the extent of π-conjugation of chromophores. Actually, TPA cross-section values have been determined for the porphyrin tapes, 11 900 GM for the dimer, 33 100 GM for the trimer, and 93 600 GM for the tetramer at 1200 nm.[19] The TPA cross section of the porphyrin sheet **3** was determined by using the open-

(17) Gouterman, M. *J. Mol. Spectrosc.* **1961**, *6*, 138.
(18) (a) Cho, H. S.; Jeong, D. H.; Cho, S.; Kim, D.; Matsuzaki, Y.; Tanaka, K.; Tsuda, A.; Osuka, A. *J. Am. Chem. Soc.* **2002**, *124*, 14642. (b) Kim, D. Y.; Ahn, T. K.; Kwon, J. H.; Kim, D.; Ikeue, T.; Aratani, N.; Osuka, A.; Shigeiwa, M.; Maeda, S. *J. Phys. Chem. A* **2005**, *109*, 2996.
(19) Ahn, T. K.; Kim, K. S.; Kim, D. Y.; Noh, S. B.; Aratani, N.; Ikeda, C.; Osuka, A.; Kim, D. *J. Am. Chem. Soc.* **2006**, *128*, 1700.

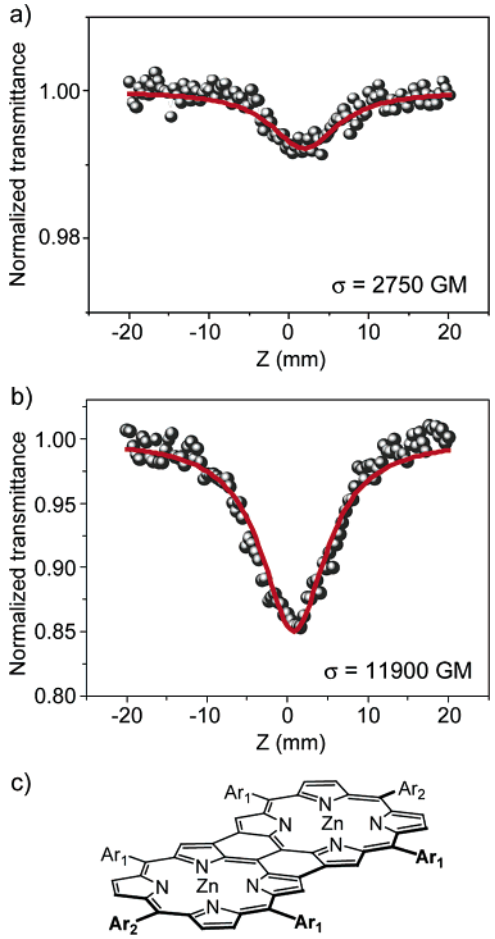

Figure 6. The open aperture *Z*-scan traces (circle) of (a) **3** and (b) fused dimer in toluene containing 1% butylamine. The sample concentrations for (a) **3** and (b) fused dimer are 0.039 and 0.165 mM, respectively. The peak irradiance at the focal point is 30 GW/cm^2. The solid lines are the best fitted curves of experimental data. (c) Molecular structure of the fused dimer (Ar_1 = *p*-nonylphenyl, Ar_2 = phenyl).

aperture *Z*-scan method with 130 fs pulses at 1600 nm where its linear absorption is almost negligible. Despite its tetrameric porphyrin constitution, the porphyrin sheet **3** exhibits a small TPA value of 2750 GM (Figure 6a), which is only ca. one-fourth of the value of the corresponding dimeric porphyrin tape (Figure 6b,c), suggesting that the electronic delocalization in **3** is quite unique, being different from those of normal porphyrins.

^{1}H NMR Studies on Supramolecular Assemblies. As described above, the conjugated π-electronic system of **3** is significantly altered from those of normal porphyrins, as highlighted by the nondegenerate HOMO and LUMO, the negative Faraday *A* terms for Band II, the slightly longer S_1-state lifetime, and the relatively small TPA value. An important structural feature of **3** is the presence of the formal planar π-conjugated COT core, which is a typical antiaromatic segment. Therefore, the influences of the planar COT moiety on the overall electronic properties of **3** are of great interest. Key questions are (1) does the COT segment really cause any paratropic ring current in **3** and (2) is the diatropic ring current in each constitutional zinc(II) porphyrin preserved or significantly perturbed by the planar COT segment? We thus examined the magnetic properties of **3** through host−guest interactions with 1,4-bis(1-methylimidazol-2-ylethynyl)benzene (**G1**) and 5,15-bis(1-methylimidazol-2-yl)-10,20-dihexylporphyrin (**G2**), which were designed to be diagonally bound on **3** as shown in Scheme 2. The distances between the coordinating two nitrogen atoms are estimated as ca. 12.4 and 11.6 Å for **G1** and **G2**, respectively, being adjusted to the calculated distance between the diagonal zinc(II) ions in **3** (11.9 Å).

Synthetic routes to **G1** and **G2** are outlined in Scheme 3. Sonogashira coupling of 1-methyl-2-iodoimidazole with trimethylsilylacetylene gave **4** in 75% yield, which was then deprotected with KOH in methanol to afford 2-ethynyl-1-methylimidazole (**5**) in 85% yield. Sonogashira coupling of **5** with 1,4-diiodobenzene provided **G1** in 29% yield. Acid-catalyzed condensation of 2-formyl-1-methylimidazole with *meso*-hexyldipyrromethane followed by oxidation with *p*-chloranil gave **G2** in 8.3% yield.[20]

Stable complexes of **3** with **G1** and **G2** were prepared by addition of excess amounts of the guest molecules to a $CHCl_3$ solution of **3**, and the resulting solutions were diluted with acetonitrile and were carefully evaporated to induce precipitation of the corresponding pure complexes. The ^{1}H NMR spectra of these complexes revealed that the stoichiometry of **3** to guest was 1:2, thus indicating the formation of **3**-(**G1**)$_2$ and **3**-(**G2**)$_2$ complexes (Scheme 2).[21] The parent ion peaks were successfully detected by high-resolution electrospray ionization mass spectroscopy (HR-ESI-MS) in a positive mode at m/z = 1774.7307 for [**3**-(**G1**)$_2$]$^{2+}$ (calcd for $[C_{228}H_{212}N_{24}Zn_4]^{2+}$ = 1774.7245) and 2126.9865 for [**3**-(**G2**)$_2$]$^{2+}$ (calcd for $[C_{272}H_{276}N_{32}Zn_4]^{2+}$ = 2126.9881), respectively (Figure 7). Curiously, the complex **3**-(**G1**)$_2$ displays a clear ^{1}H NMR spectrum, in which the 1,4-phenylene protons (H^d) appear at 10.95 ppm, being 3.78 ppm downfield shifted from its original chemical shift, whereas the imidazolyl protons (H^a, H^b, and H^c) exhibit reverse upfield shifts (Figure 8). The complexation-induced shifts (CIS), which are defined as the difference of chemical shifts of signals of bound guests and free guests (CIS = $\delta_{bound} - \delta_{free}$), are summarized in Chart 1. The ^{1}H NMR spectrum of **3**-(**G2**)$_2$ is relatively simple, exhibiting sharp signals, but some of the peaks (H^e and the aryl protons of **3**, and the β-protons of **3** and solvent protons) are severely overlapped. To distinguish each proton signal in the complex **3**-(**G2**)$_2$, the ^{1}H NMR spectrum has been examined at various temperatures (Supporting Information). The assignment of the ^{1}H NMR signals of the complexes relies on the comprehensive 2D-COSY and 2D-NOESY spectra as well as proton−deuterium exchange experiments by addition of D_2O. The latter experiments allowed for the assignment of the porphyrin inner NH protons of **G2**. Interestingly, the porphyrin inner NH protons show the largest downfield shift (CIS = +5.29 ppm), whereas the imidazolyl protons (H^a, H^b, and H^c) and the side-chain hexyl protons (H^g and H^h) exhibit more or less upfield shifts (Chart 1). These observations revealed a strong deshielding magnetic effect of the central COT core but a weak diatropic ring current for the local zinc(II) porphyrin subunits.

DFT Calculation. To understand the anomalous shielding and deshielding magnetic effects of **3**, theoretical calculations were performed for the meso-unsubstituted porphyrin sheet **3**$_H$ and its free-base form **3**$_H$FB, which gave respective energy minimized structures and nucleus-independent chemical shifts (NICS).[22] Structures were optimized with Becke's three-

(20) Ikeda, C.; Fujiwara, E.; Satake, A.; Kobuke, Y. *Chem. Commun.* **2003**, 616.
(21) Screen, T. E. O.; Thorne, J. R. G.; Denning, R. G.; Bucknall, D. G.; Anderson, H. L. *J. Am. Chem. Soc.* **2002**, *124*, 9712.

Scheme 2. Schematic Representation of Complexation of **3** with Two Bisimidazolyl Guest Molecules

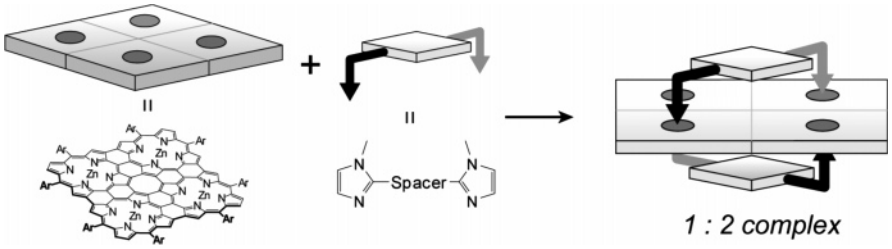

Scheme 3. Syntheses of **G1** and **G2**[a]

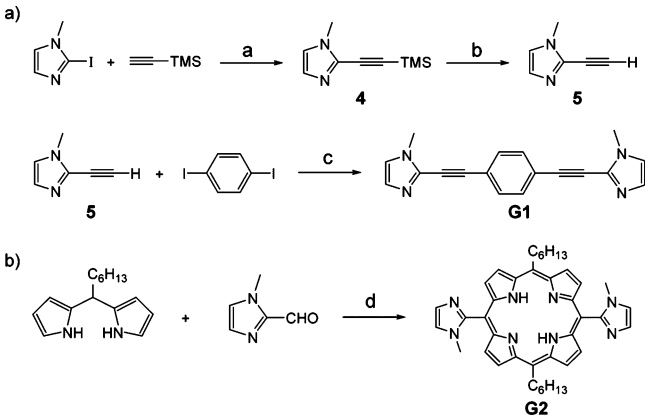

[a] Conditions: (a) $Pd(PPh_3)_2Cl_2$, CuI, Et_3N, THF, 75%; (b) KOH, MeOH, 85%; (c) $Pd(PPh_3)_2Cl_2$, CuI, Et_3N, THF, 29%; (d) (i) TFA, $CHCl_3$, (ii) *p*-chloranil, then Et_3N, 8.3%.

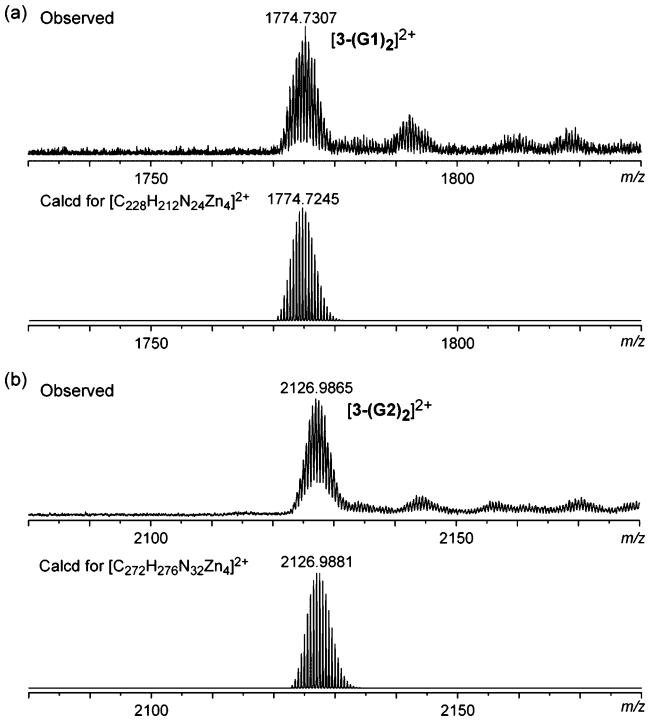

Figure 7. Observed and calculated ESI mass spectra of (a) **3**-(**G1**)$_2$ and (b) **3**-(**G2**)$_2$.

parameter hybrid exchange functional and the Lee−Yang−Parr correlation functional (B3LYP), employing the LANL2DZ basis set for zinc and 6-31G* for the rest of the atoms (denoted as

Chart 1. Molecular Structures and CIS (ppm) of Proton Signals of (a) **G1** and (b) **G2** at Room Temperature, and Expected Structures of (c) **3**-(**G1**)$_2$ Complex, and (d) **3**-(**G2**)$_2$ Complex[a]

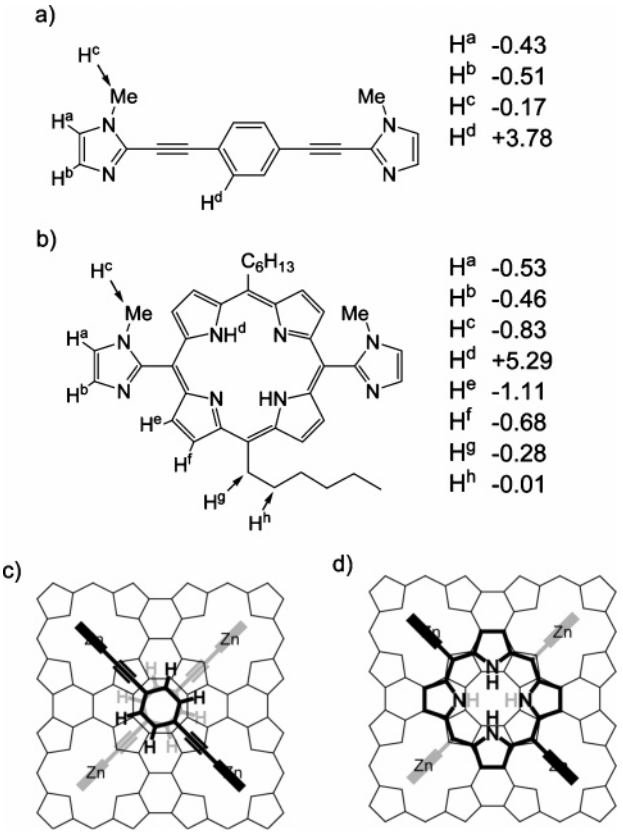

[a] In (c) and (d), bold line drawings are on **3** and gray line drawings are back of **3**.

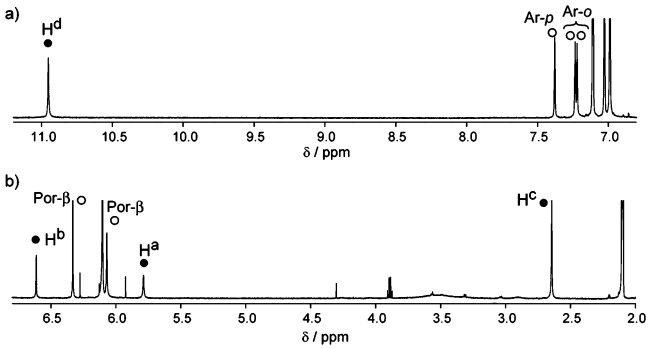

Figure 8. ^{1}H NMR spectra of **3**-(**G1**)$_2$ in toluene-d_8. (a) Low-field region and (b) high-field region. Open and filled circles indicate the signals of **3** and **G1** in the complex, respectively.

631LAN). The optimized structures have revealed that both $\mathbf{3}_H$ and $\mathbf{3}_H$FB take perfectly square-planar conformations, in which the bond length alternation (ΔR) in the COT moiety is small,

(22) (a) Schleyer, P. v. R.; Maerker, C.; Dransfeld, A.; Jiao, H.; Hommes, N. J. R. v. E. *J. Am. Chem. Soc.* **1996**, *118*, 6317. (b) Chen, Z.; Wannere, C. S.; Corminboeuf, C.; Puchta, R.; Schleyer, P. v. R. *Chem. Rev.* **2005**, *105*, 3842.

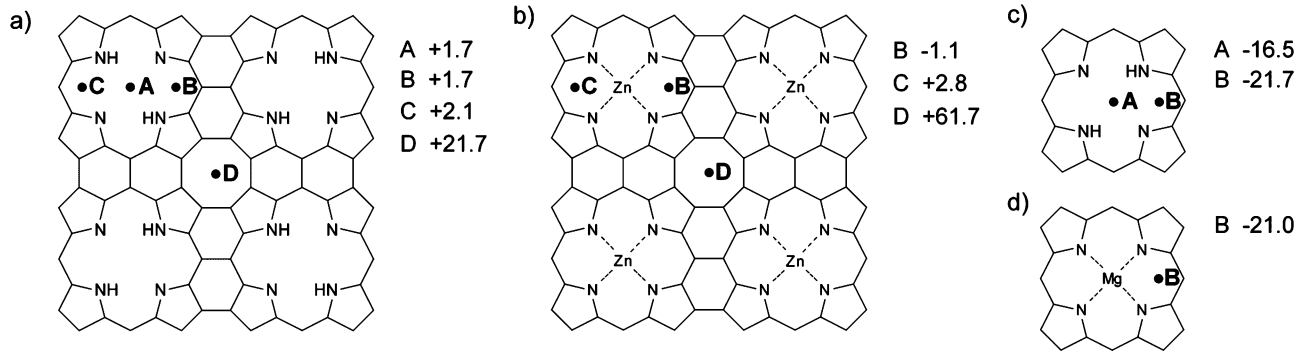

Figure 9. NICS values (ppm) of (a) $\mathbf{3}_{H}$FB, (b) $\mathbf{3}_{H}$, (c) porphine, and (d) magnesium(II) porphine. Point A was defined as the center of the porphyrin internal cross, and points B and C were defined as the mean points of two adjacent CN bonds.[23]

$\Delta R = 0.052$ and 0.039 Å for $\mathbf{3}_{H}$ and $\mathbf{3}_{H}$FB, respectively, because the bond length of C−C bonds between the pyrroles and the bond length of C−C bonds in the pyrroles are similar, being 1.392 and 1.444 Å for $\mathbf{3}_{H}$ and 1.401 and 1.440 Å for $\mathbf{3}_{H}$FB, respectively. On the basis of these energy-minimized structures, NICS values have been calculated at the GIAO-B3LYP/631LAN level for $\mathbf{3}_{H}$FB and $\mathbf{3}_{H}$ as shown in Figure 9. Inside the porphyrin, the NICS values have been calculated to be + 1.7, +1.7, and +2.1 for points A, B, and C in Figure 9a, suggesting the aromatic character of porphyrin is substantially weakened and almost lost in $\mathbf{3}_{H}$FB.[23] Because the NICS calculation in the center of porphyrin units in $\mathbf{3}_{H}$ is impossible due to the presence of zinc(II) ion, the values at points B and C have been calculated to be −1.1 and +2.8, respectively (Figure 9b). These values are exceptionally small as compared to those calculated for porphine and magnesium(II) porphine (Figure 9c,d),[23] also suggesting the disappearance of the aromatic character for the porphyrin ring in $\mathbf{3}_{H}$. On the other hand, the NICS values of the center of the COT core have been calculated to be +21.7 for $\mathbf{3}_{H}$FB and +61.7 for $\mathbf{3}_{H}$, which are comparable to or larger than a NICS value (+29.2) calculated for a hypothetical D_{4h} cyclooctatetraene that is a typical antiaromatic species.[22a,24,25] These calculations indicate that there is a strong paratropic ring current along the COT core that propagates to the whole π-network of **3**, affecting the local 18π aromatic porphyrin systems, whereas the four zinc(II) porphyrin subunits still preserve weak diatropic ring currents. As a consequence of the two opposite effects, small upfield shifts are observed for the imidazolyl protons coordinating to the zinc(II) centers.

Summary

The directly fused tetrameric porphyrin sheet **3** that was synthesized from the directly linked porphyrin ring **2** exhibits unusual properties including the broad absorption spectrum, the negative Faraday *A* terms for Band II, the slightly longer S_1-state lifetime, and the relatively small TPA value. The calculations on TDHF-ZINDO/S revealed their nondegenerate HOMO and LUMO orbitals. A strong paratropic ring current was detected above the COT core, while weak diatropic ring currents are preserved at each local zinc(II) porphyrin. These anomalous properties are likely arising from the COT segment, which is enforced to be planar by the direct fusion of four zinc(II) porphyrins. As such, conjugation of a strongly antiaromatic segment with porphyrin may be a general and effective way to alter the electronic properties of porphyrin, which will lead to creation of novel porphyrinoid. Along this line, our efforts are in progress toward exploration of novel porphyrinic molecules.

Experimental Section

General Information. All reagents and solvents were of commercial reagent grade and were used without further purification except where noted. Dry toluene and Et_3N were obtained by distilling over CaH_2. Dry THF was obtained by distilling over sodium benzophenone ketyl. ^{1}H NMR spectra were recorded on a JEOL ECA-delta-600 spectrometer, and chemical shifts were reported as the delta scale in ppm relative to $CHCl_3$ ($\delta = 7.26$ ppm) or methyl protons of toluene ($\delta = 2.10$ ppm). Mass spectra were recorded on a Shimadzu/KRATOS KOMPACT MALDI 4 spectrometer, using the positive-MALDI ionization method with 9-nitroanthracene (9NA) matrix, or on a BRUCKER microTOF using positive-ion mode, and CH_3CN as a solvent.

Synthesis. Porphyrin Sheet 3. To a solution of **2** (1.53 mg, 0.51 μmol) in dry toluene (3 mL) were added DDQ (3.5 mg, 1.5 μmol) and $Sc(OTf)_3$ (10.3 mg, 1.5 μmol), and the resulting mixture was stirred for 5 h at 55 °C with shielding from light under Ar atmosphere. The reaction mixture was diluted with THF and was passed through an alumina column with THF. After evaporation of the solvent, the residue was dissolved in THF, poured on alumina column, and washed with THF to remove impurities. A purple fraction that still remained on the alumina column was then eluted with toluene and butylamine alternatively. This procedure was repeated twice or three times. The combined eluant was evaporated, and the residue was recrystallized from CH_2Cl_2/CH_3CN to afford black solids of **3**·4(butylamine) (1.28 mg, 0.39 μmol, 77%). ^{1}H NMR ($CDCl_3$) δ 7.29 (t, $J = 1.6$ Hz, 8H, Ar-*p*), 7.01 (d, $J = 1.9$ Hz, 16H, Ar-*o*), 6.14 (s, 8H, β), 5.98 (s, 8H, β), and 1.22 (s, 144H, ^{t}Bu) ppm; MALDI-TOF MS *m*/*z* 2977.4, calcd for $C_{192}H_{184}N_{16}Zn_4$ 2977.2; UV−vis ($CHCl_3$/5% *n*-$BuNH_2$) $\lambda_{max}(\epsilon) = 521$ (96 000), 639 (42 000), 756 (77 000), and 1256 (9700) nm.

2-Trimethylsilylethynyl-1-methylimidazole (4). To a solution of 2-iodo-1-methylimidazole (1.0 g, 4.8 mmol), $Pd(PPh_3)_2Cl_2$ (336 mg, 0.48 mmol), and CuI (91 mg, 0.48 mmol) in dry THF (3 mL) and Et_3N (13 mL) was added a solution of trimethylsilylacetylene (2.4 g, 24 mmol) in dry THF (2 mL). The solution was deoxygenated via freeze−pump−thaw cycles and was stirred at 35 °C under Ar atmosphere. After 9 h, the resulting mixture was filtrated and evaporated. The residue was extracted with ethyl acetate and washed with water. The combined organic layer was dried over Na_2SO_4 and evaporated. Silica gel column chromatography (ethyl acetate:hexane,

(23) Cyrañski, M. K.; Krygowski, T. M.; Wisiorowski, M.; Hommes, N. J. R. v. E.; Schleyer, P. v. R. *Angew. Chem., Int. Ed.* **1998**, *37*, 177.
(24) About planar COT and its derivatives: (a) Klärner, F.-G. *Angew. Chem., Int. Ed*. **2001**, *40*, 3977 and references therein. (b) Matsuura, A.; Komatsu, K. *J. Am. Chem. Soc.* **2001**, *123*, 1768. (c) Fowler, P. W.; Havenith, R. W. A.; Jenneskens, L. W.; Soncini, A.; Steiner, E. *Angew. Chem., Int. Ed.* **2002**, *41*, 1558.
(25) A large difference between the calculated NICS vales for the COT center of $\mathbf{3}_{H}$ and $\mathbf{3}_{H}$FB is difficult to explain but may be ascribed due to symmetry difference.

2:1) of the residue gave **4** as a pale yellow oil (640 mg, 3.6 mmol, 75%). ^{1}H NMR ($CDCl_3$) δ 7.00 (s, 1H, Im), 6.86 (s, 1H, Im), 3.70 (s, 3H, Me), and 0.25 (s, 9H, TMS) ppm.

2-Ethynyl-1-methylimidazole (5). To a solution of 2-trimethylsilylethynyl-1-methylimidazole (**4**) (300 mg, 1.7 mmol) in MeOH (15 mL) was added a small portion of aqueous KOH solution. After being stirred for 30 min at room temperature, the solution was diluted with water and was extracted with ethyl acetate. The combined organic layer was dried over Na_2SO_4 and evaporated. Silica gel column chromatography (ethyl acetate:hexane, 3:1) gave **7** as a pale yellow oil (152 mg, 1.4 mmol, 85%). ^{1}H NMR ($CDCl_3$) δ 7.04 (s, 1H, Im), 6.90 (s, 1H, Im), 3,74 (s, 3H, Me), and 3.31 (s, 1H, C≡CH) ppm.

1,4-Bis(1-methylimidazol-2-ylethynyl)benzene (G1). To a mixture of 1,4-diiodobenzene (40 mg, 0.12 mmol), $Pd(PPh_3)_2Cl_2$ (25 mg, 0.031 mmol), and CuI (6.9 mg, 0.031 mmol) was added a solution of **5** (32 mg, 0.31 mmol) in dry Et_3N (1 mL) and dry THF (1 mL). The solution was deoxygenated via freeze−pump−thaw cycles and was stirred at room temperature under Ar atmosphere. After 1 day, the resulting mixture was filtrated and evaporated. The residue was extracted with ethyl acetate and washed with water. The combined organic layer was dried over Na_2SO_4 and evaporated. Silica gel column chromatography (ethyl acetate) of the residue gave **G1** as yellow brown solids (10.1 mg, 0.035 mmol, 29%). ^{1}H NMR ($CDCl_3$) δ 7.55 (s, 4H, Ph), 7.11 (s, 2H, Im), 6.96 (s, 2H, Im), and 3.80 (s, 6H, Me) ppm; (toluene-d_8) δ 7.17 (s, 4H, Ph), 7.12 (s, 2H, Im), 6.23 (s, 2H, Im), and 2.91 (s, 6H, Me) ppm. ESI-MS *m*/*z* 287.120 $[M + H]^+$; calcd for $C_{18}H_{15}N_4^+$, *m*/*z* 287.129.

5,15-Bis(1-methylimidozol-2-yl)-10,20-dihexylporphyrin (G2). 2-Formyl-1-methylimidazole (200 mg, 1.8 mmol), *meso*-hexyldipyrromethane (418 mg, 1.8 mmol), and NaCl (53 mg, 0.9 mmol) were dissolved in $CHCl_3$ (189 mL). After the solution was purged with N_2 for 15 min, TFA (0.2 mL, 2.7 mmol) was added, and the resulting solution was stirred at room temperature with shielding from light under nitrogen atmosphere. After 6 h, *p*-chloranil (664 mg, 2.7 mmol) was added to the reaction mixture, and the solution was stirred for 12 h. The reaction mixture was then neutralized with triethylamine, and the solvent was evaporated. The residue was dissolved in $CHCl_3$ and passed through a silica gel column with $CHCl_3$ to $CHCl_3$/acetone (10:3) as eluents. This procedure was repeated three times to give pure **G2** as red-purple solids (48 mg, 0.075 mmol, 8.3%). ^{1}H NMR (toluene-d_8) δ 9.26, 9.23 (each d, J = 4.8 Hz, 4H, Por-β), 8.83, 8.76 (each d, J = 4.6 Hz, 4H, Por-β), 7.74, 7.67 (each s, 2H, Im-H_4), 6.94, 6.88 (each s, 2H, Im-H_5), 4.77, 4.73 (each m, 4H, Hex-α), 2.83, 2.80 (each s, 6H, Im−N−Me), 2.48, 2.43 (each m, 4H, Hex-β), 1.68 (m, 4H × 2, Hex-γ), 1.42 (m, 4H × 2, Hex-δ), 1.36 (m, 4H × 2, Hex-ϵ), 0.95 (m, 6H × 2, Hex-Me), −2.40, and −2.45 (each br, 2H, Por-NH) ppm; HR-ESI-MS *m*/*z* 639.3924 $[M + H]^+$; calcd for $C_{40}H_{47}N_8^+$, *m*/*z* 639.3918.

STM Measurements. Clean flat Cu(100) surfaces were obtained by Ar^+-ion sputtering and annealing (580 °C) cycles for a substrate. The porphyrin sheet molecules dissolved into $CHCl_3$ were deposited by spraying ca. 0.5 μL of the solution onto the substrate in a vacuum (10^{-6} mbar) using a pulse injection method, which is suited for deposition of large fragile molecules with escaping decomposition often encountered in sample deposition from the gas phase. In-situ STM measurements were performed at room temperature in ultrahigh vacuum ($<10^{-10}$ mbar) with a home-built STM by using an electrochemical etched Pt/Ir tip. STM image was obtained in constant height mode.

Steady-State UV−Vis Absorption Spectroscopy. The samples were prepared in micromolar concentrations in $CHCl_3$ (spectroscopic grade). Absorption spectra were obtained with a Shimadzu UV-3100PC spectrometer at room temperature.

Transient Absorption Spectroscopy. The dual-beam femtosecond time-resolved transient absorption spectrometer consisted of a self-mode-locked femtosecond Ti:sapphire oscillator (Coherent, MIRA), a Ti:sapphire regenerative amplifier (Clark MXR model TRA-1000) that was pumped by a Q-switched Nd:YAG laser (Clark MXR model ORC-1000), a pulse stretcher/compressor, an optical parametric amplifier (Clark MXR OPA), and an optical detection system. A femtosecond Ti:sapphire oscillator pumped by a cw Nd:YVO_4 laser (Coherent, Verdi) produces a train of ∼80-fs mode-locked pulses with an averaged power of 650 mW at 800 nm. The amplified output beam regenerated by chirped pulse amplification (CPA) had a pulse width of ca. 150 fs and a power of ca. 1 W at a repetition rate of 1 kHz, which was divided into two parts by a 1:1 beam splitter. One part was color-tuned for the pump beam by an optical parametric generation and amplification (OPG-OPA). The resulting laser pulse had a temporal width of ∼150 fs in the vis/IR range. The pump beam was focused to a spot diameter of ∼1 mm, and the laser fluence was adjusted, using a variable neutral-density filter. The other part was focused onto a flowing water cell to generate a white-light continuum, which was again split into two parts. One part of the white-light continuum was overlapped with the pump beam at the sample to probe the transient, while the other part of the white-light continuum was passed through the sample without overlapping the pump beam. The time delay between pump and probe beams was controlled by making the pump beam travel along a variable optical delay line. The white-light continuum beams after the sample were sent through an appropriate interference filter and then were detected by two photodiodes. The outputs from the two photodiodes at the selected wavelength were processed by a combination of a boxcar averager and a lock-in amplifier, to calculate the absorption difference at the desired time delay between pump and probe pulses. Two-photon absorption cross sections were measured by an open-aperture *Z*-scan method using the setup reported elsewhere.[18b]

Magnetic Circular Dichroism (MCD) Spectroscopy. The MCD spectrum was recorded in the UV−vis−near-IR region (300−900 nm) with a JASCO J-725 spectrodichrometer equipped with a JASCO electromagnet that produces parallel and antiparallel magnetic fields of up to 1.09 T, and in the near-IR region (700−2000 nm) with a JASCO J-730 spectrodichrometer equipped with a JASCO electromagnet that produces magnetic fields of up to 1.5 T. Pyridine-d_5 was used as solvent to eliminate solvent absorption bands in the near-IR region. The MCD spectrum was combined in a region where there were no intense absorption bands. The magnitude of the MCD signal is expressed in terms of molar ellipticity per tesla $[\theta]_M$ deg mol^{-1} dm^3 cm^{-1} T^{-1}.

Computational Details. All calculations were carried out using the Gaussian 03 program.[26] All structures were optimized with Becke's three-parameter hybrid exchange functional and the Lee−Yang−Parr correlation functional (B3LYP)[27] without symmetry restriction, employing the LANL2DZ basis set for zinc atom, and 6-31G* basis set for the other atoms (denoted as 631LAN). The NICS values were obtained with the GIAO method at B3LYP/631LAN level. The ring centers were designated at the nonweighted means of the carbon and nitrogen coordinates on the conjugate pathways. The ground-state structure of **3** with D_{4h} symmetry was optimized at the level of B3LYP/6-31G*, where the *tert*-butyl groups were omitted and replaced with hydrogen atoms. With this optimized structure, the 40 excitation energies and oscillator strengths were calculated using time-dependent Hartree−Fock theory (TDHF) with ZINDO/S Hamiltonian.

Acknowledgment. The work at Kyoto was partly supported by a Grant-in-Aid for Scientific Research on Priority Area (No. 16033231, Reaction Control of Dynamic Complexes) from the Ministry of Education, Culture, Sports, Science, and Technology, Japan, and 21st Century COE on Kyoto University Alliance for Chemistry. The work at Tohoku was supported by the COE project, Giant Molecules and Complex Systems, 2005, and a

(26) Frisch, M. J.; et al. *Gaussian 03*, revision B.05; Gaussian, Inc.: Pittsburgh, PA, 2003.
(27) (a) Becke, A. D. *Phys. Rev. A* **1988**, *38*, 3098−3100. (b) Lee, C.; Yang, W.; Parr, R. G. *Phys. Rev. B* **1988**, *37*, 785−789.

Grant-in-Aid for Scientific Research (B) No. 17350063 from the Ministry of Education, Culture, Sports, Science, and Technology, Japan. The work at Yonsei was supported by the National Creative Research Initiatives Program of the Ministry of Science and Technology of Korea. Y.N. thanks the JSPS fellowship for Young Scientists. We thank Prof. Masanobu Uchiyama and Taniyuki Furuyama for near-IR MCD measurements.

Supporting Information Available: Absorption spectrum, details of MO calculation, measurement of two-photon absorption cross section, binding experiments of **3** with **G1** and **G2**, details of structure optimization calculations, and full citation for ref 26. This material is available free of charge via the Internet at http://pubs.acs.org.

JA057812L